Effect of different co-solvents on biodiesel production from various low-cost feedstocks using Sr–Al double oxides

Ambat Indu, Srivastava Varsha, Iftekhar Sidra, Haapaniemi Esa, Sillanpää Mika

DOI: 10.1016/j.renene.2019.08.061

Effect of different co-solvents on biodiesel production from various low-cost feedstocks using Sr-Al double oxides

Indu Ambat [a]*, Varsha Srivastava [a], Sidra Iftekhar [a], Esa Haapaniemi [b], Mika Sillanpää [a]

[a] Department of Green Chemistry, School of Engineering Science, Lappeenranta University of Technology, Sammonkatu 12, FI-50130 Mikkeli, Finland

[b] Department of Organic Chemistry, University of Jyväskylä, Finland

*Corresponding Author (E-mail: indu.ambat@lut.fi)

Abstract

The main objective of the present paper comprises the investigation of biodiesel production from low-cost feedstock such as lard oil and waste cooking oil (WCO) using Sr-Al double oxides. Nanocatalyst was characterised FTIR, XRD, SEM, TEM, BET and XPS. The Sr:Al with 3:1 molar ratio showed the best catalytic activity in the conversion of both oils to fatty acid methyl ester. The effect of acetone and tetrahydrofuran (THF) as a co-solvent for transesterification were compared and the best result was obtained with 5 % THF. The mutual effect of the nanocatalyst and co-solvent on biodiesel production was investigated. The characterisation of biodiesel synthesised from lard oil and WCO was performed with GC-MS, ^{1}H and ^{13}C NMR. Moreover, the optimum reaction parameters for transesterification reaction was analysed and the yield was determined by ^{1}H NMR. The maximum yield of 99.7% and 99.4% of lard oil methyl ester and WCO biodiesel were observed with a 0.9 wt% catalyst amount, 1:5.5 oil to methanol ratio in a reaction time of 45 minutes at 50°C and 60°C, respectively. The properties of biodiesel from lard oil and WCO were determined by the EN 14214 method. The regeneration, characterization and reusability of regenerated catalyst was observed.

Keywords: Biodiesel, lard oil, transesterification, Sr-Al double oxides, waste cooking oil

1. Introduction

Currently, the perpetual concern is the depletion of conventional fuels due to the massive utilisation of fossil fuels. Moreover, the excessive use of petroleum products leads to global warming and environmental pollution. Due to these issues, there is a need for an alternative fuel [1,2]. Biodiesel is a suitable alternative fuel due to its biodegradability, non-toxicity, renewability, lower emission of sulfur and carbon dioxide and eco-friendly nature [3-5].

Biodiesel comprises fatty acid methyl esters, commonly produced by the transesterification of fats or oils using methanol in the presence of a catalyst [3,6,7]. The bottleneck issues associated with the transesterification process are the selection of suitable feedstock, catalyst and an efficient method for the biodiesel production [2],[8-10]. The selection of feedstock for biodiesel production plays an important role in the determination of fuel cost. Hence, keeping this point in mind the raw materials used in the present work includes lard oil and waste cooking oil. Furthermore, the application of nanocatalytic technology for biodiesel production helps to improve catalytic activity, reusability and stability [2, 5, 11]. The problems involved in the transesterification reaction such as a lower rate of reaction, poor phase separation and soap formation can be resolved with the help of the co-solvent method [8-10] [12].

The present work was targeted to synthesise Sr-Al double oxides with four different molar ratios metal ions. The application of Sr-Al double oxides for biodiesel synthesis is rather scanty and not well explored. Moreover, heterogeneous catalyst offers better stability and reusability with lower cost in comparison with homogenous or biocatalyst [11]. Later, synthesised Sr-Al double oxides were screened for biodiesel production and the catalyst showed the best catalytic activity when used for the further reaction. Furthermore, as the co-solvent plays an important role in the enhancement of biodiesel yield and, therefore, the role of a different co-solvent with Sr-Al nanocatalyst in biodiesel synthesis was also studied in the present work. The combined effect of the nanocatalyst and co-solvent in biodiesel production from different feedstock was investigated. Furthermore, to the best of our knowledge, the transesterification of lard oil and waste cooking oil (WCO) using Sr-Al nanocatalysts and co-solvent have not been investigated. The selection of oil was due to its low cost and availability.

The characterisation of synthesised nanocatalyst was done using Fourier transform infrared spectroscopy (FTIR), Scanning electron microscopy (SEM), X-ray diffraction (XRD), Transmission electron microscopy (TEM) and Brunauer-Emmett-Teller (BET) and X-ray photoelectron spectroscopy (XPS). The biodiesel obtained after a transesterification reaction was analysed by gas chromatography with mass spectrometry (GC-MS), ^{1}H and ^{13}C nuclear magnetic resonance (NMR). The reaction parameters such as co-solvent percentage, reaction temperature, molar ratio of oil and methanol, catalyst amount and reaction time were analysed. The physic-chemical properties of obtained biodiesel was determined using EN 14214 method.

2. Experimental

2.1 Chemicals

Lard oil (FFA%= 0.423) and waste cooking oil (FFA%= 0.634) were obtained from Sigma-Aldrich and household oil waste, respectively. The aluminium nitrate nonahydrate, citric acid monohydrate acs reagent, methanol, acetone, tetrahydrofuran (THF) anhydrous and heptane were purchased from Sigma-Aldrich. The strontium nitrate was obtained from VWR International. All the chemicals were of analytical grade.

2.2 Synthesis and screening of the catalyst

Four different samples of Sr-Al mixed oxides were synthesised using the sol-gel citrate method. The samples were prepared by mixing metal nitrate of Sr / Al in different molar ratios of 1:1, 1:0.51, 1:0.33, and 1:0.25 respectively and stirred for 1 h. Thereafter, stoichiometric amount of citric acid was added to metal nitrate solution followed by additional stirring for 1 h [45]. The molar ratios of citric acid to total metal cations concentration were kept 2[46]. The mixture was then heated over 100°C until a clear transparent gel was obtained. The resultant gel was dried at 110°C overnight and then dried gel was grounded to get fine powder which was further calcined at 700°C for 5 h.

The catalysts were screened for fatty acid methyl ester (FAME) production from lard oil and WCO.

2.3 Characterisation of catalyst

XRD patterns of synthesised catalyst were captured with PANalytical – Empyrean X-ray diffractometer over a 2θ range of 10-120º with an X-ray source Co-Kα of 0.178 nm at 40 mA and 40 kV. FTIR (Vertex 70 model by Bruker) used to analyse functional groups of synthesised catalyst by capturing IR spectra from 400 to 4000 cm^{-1}. SEM images of nanocatalysts were obtained by spreading the sample on colloidal graphite with 5 kV accelerating voltage (SEM, Hitachi SU3500). TEM images of the samples were captured using HT7700 (Hitachi). For attaining TEM images, the nanocatalyst was dispersed in ethanol and sonicated for 25 min and a drop of suspension was added to the carbon coated copper grid. Surface area, pore diameter and pore volume of synthesised catalysts were determined using BET surface area analyser (BET, Micromeritics Tristar II plus). Prior to performing BET analysis, the catalyst samples were degassed at 35°C overnight to remove the moisture from the samples. The surface composition and the binding energies of elements in nanocatalysts were examined by ESCALAB 250 model XPS with an Al-K X-ray source of 1486.6 eV.

2.4 *Reaction procedure*

Lard and waste cooking oil were used as feedstock for biodiesel production. The fatty acid methyl ester production from each oil using different ratios of Sr-Al double oxides was done in a 250 ml three neck round bottom flask with mechanical stirrer and reflux condenser at 60°C by mixing methanol to oil in a 5:1 molar ratio and with 2.5wt% of each catalyst for 120 min. The various methanol to oil ratios were reported for transesterification studies and theoretically 3: 1 molar ratio is enough for transesterification reaction [11, 35, 36, 37]. All the reactions were conducted in triplicates. The phase separation of fatty acid methyl ester, glycerol and catalyst were achieved by the centrifugation of the samples after each reaction. The selection of the best catalyst for further studies was completed by analysing the obtained FAME concentration. In

addition, excess methanol in ester phase and catalyst after the reaction were recovered after the transesterification reaction. The separated catalyst was washed with methanol and heptane to remove impurities. After washing, the catalyst reactivation was achieved by drying the recovered catalyst at 60°C followed by calcination at 700°C for 5 h.

As an extension of this work, the influence of a different co-solvent like acetone and THF on biodiesel production was investigated. The transesterification reactions were conducted for the comparison of co-solvents by varying its amount from 5 to 20 wt % in each reaction with the best catalyst obtained after the screening procedure. The resulting optimised amount of the best co-solvent with the greatest performing nanocatalyst was used for further biodiesel production studies.

2.5 Analytical methods

The biodiesel attained after the transesterification reaction of lard and WCO was analysed by GC-MS (Agilent-GC6890N, MS 5975) with Agilent DB-wax FAME analysis GC column dimensions 30 m, 0.25 mm, 0.25 µm. The inlet temperature was 250°C and the oven temperature was programmed at 50°C for 1 min and it raises at the rate of 25°C/min to 200°C and 3°C/min to 230°C and then it was held for 23 min. Moreover, ^{1}H and ^{13}C NMR (Bruker) were used for the estimation of fatty acid esters content and conformation of esters in each sample, respectively. For NMR analysis, fatty acid methyl esters were examined by ^{1}H NMR and ^{13}C NMR at 400 MHz with $CDCl_3$ as a solvent. The percentage conversion of oil to fatty acid methyl esters (C%) and biodiesel yield are determined by equation 1 and 2, given below [11,37].

$$C(\%) = \frac{2 \times Intergration\ value\ of\ protons\ of\ methyl\ ester}{3 \times Intergraton\ value\ of\ methyl\ protons} \times 100 \quad (Eq.1)$$

$$Biodiesel\ yield\ (\%) = \frac{mass\ of\ biodiesel}{mass\ of\ oil} \times 100 \quad (Eq.2)$$

158

159 However, the biodiesel production was also affected by the reaction parameters
160 such as the amount of catalyst, oil to methanol ratio, reaction temperature and reaction
161 time.

162 **3. Result and discussion**

163

164 *3.1. Screening and selection of nanocatalyst for biodiesel production*

165

166 The catalytic performance of different molar ratio of Sr:Al catalyst was analysed for
167 the biodiesel production from waste cooking oil and lard oil. The catalytic activity of each
168 catalyst and the viscosity of different FAME samples was indicated in Table 1. The high
169 catalytic activity of Sr:Al with 1.0.33 molar ratio is due to the optimum loading of
170 aluminium ions and strontium ions to nanocatalyst, which offers a proper interaction
171 between the components of the catalyst. Hence, the appropriate structure of the catalyst
172 provides sufficient active sites for the fatty acids to bind with the nanocatalysts.
173 Moreover, only the biodiesel obtained using Sr:Al with molar ratio 1:0.51 and 1:0.33
174 were within the EN ISO 3104 limits. Considering the following results, Sr:Al with molar
175 ratio 1:0.33 catalyst was chosen for further optimisation studies. Thereafter, Sr:Al with
176 molar ratio 1:0.33 denoted as Sr: 0.33Al.

177

178

179 **Table 1.** The efficiency of various catalyst for transesterification

180

181

No.	**Catalyst**	**Molar ratio**	**Biodiesel yield%**		**Viscosity at 40°C mm^2/s**	
			Lard oil	WCO	Lard oil (FAME)	WCO (FAME)

1	Sr :Al	1:1	71.25	66.98	5.02	5.77
2	Sr:Al	1:0.51	80.93	79.89	4.82	4.76
3	Sr:Al	1:0.33	85.09	83.41	4.37	4.56
4	Sr:Al	1:0.25	69.42	62.23	5.96	6.23

182
183
184 *3.2. Characterisation of catalyst*
185
186 The IR bands of Sr: 0.33Al and regenerated Sr: 0.33Al were shown in Fig. 1. The
187 spectra clearly demonstrate the intensity of the IR band and were lower in regenerated Sr:
188 0.33Al compared to Sr: 0.33Al . The FTIR peaks in the region of 445 cm^{-1} to 602 cm^{-1} of
189 the spectrum indicates the frequency vibrations of AlO_6 groups. Moreover, the peaks
190 observed around 723 cm^{-1} to 872 cm^{-1} corresponding to the stretching and vibration of
191 AlO_4 [13,14]. The band at 1440.64 cm^{-1} indicates the presence of Sr-O vibrations. The
192 bending vibrations of OH groups and water molecule crystallisation correspond to the IR
193 spectra of about 3,400 cm^{-1}, 3,600 cm^{-1} and 1,640 cm^{-1}, respectively [13, 15].

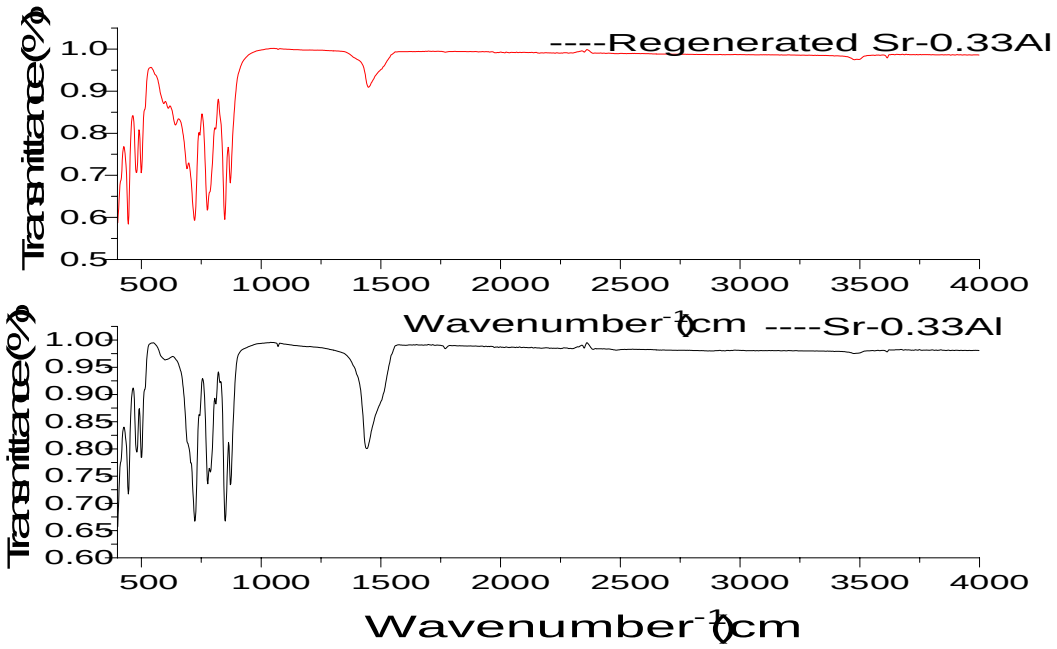

Fig. 1. FTIR spectra of Sr: 0.33Al and regenerated Sr: 0.33Al

Fig. 2 shows the strong and fine XRD pattern of Sr:Al double oxides and regenerated Sr:0.33Al over the 10-120º attribute to the crystalline nature of the synthesised nanocatalyst. The X-ray diffraction patterns at 37.1º, 45.8º, 56º, 57.1º, 58.6º, 67.1º were consigned to the typical peaks of $Sr_3Al_2O_6$ and show as a match to the earlier report in JCPDS file No. 24-1187. The $Sr_3Al_2O_6$, termed as a superstructure of the nanocatalysts, ABO_3 [41]. The less intense diffraction patterns around 18º, 24.3º, 29.9º, 34.9º 40.5º, 49.9º, 53.6º, 60.5º, 70.24º indicate the slight existence of $SrCO_3$ [13,16]. Concisely, the diffractogram shows that a clear difference happened to Sr: 0.33Al after transesterification. In comparison with Sr: 0.33Al, XRD patterns at 18º, 24º, 40.5º, 58.6º and 70.2º disappeared in the regenerated Sr: 0.33Al and the intensity of rest of the peaks was reduced. This might be due to slight leaching of Sr and Al ions after reuse of the catalyst.

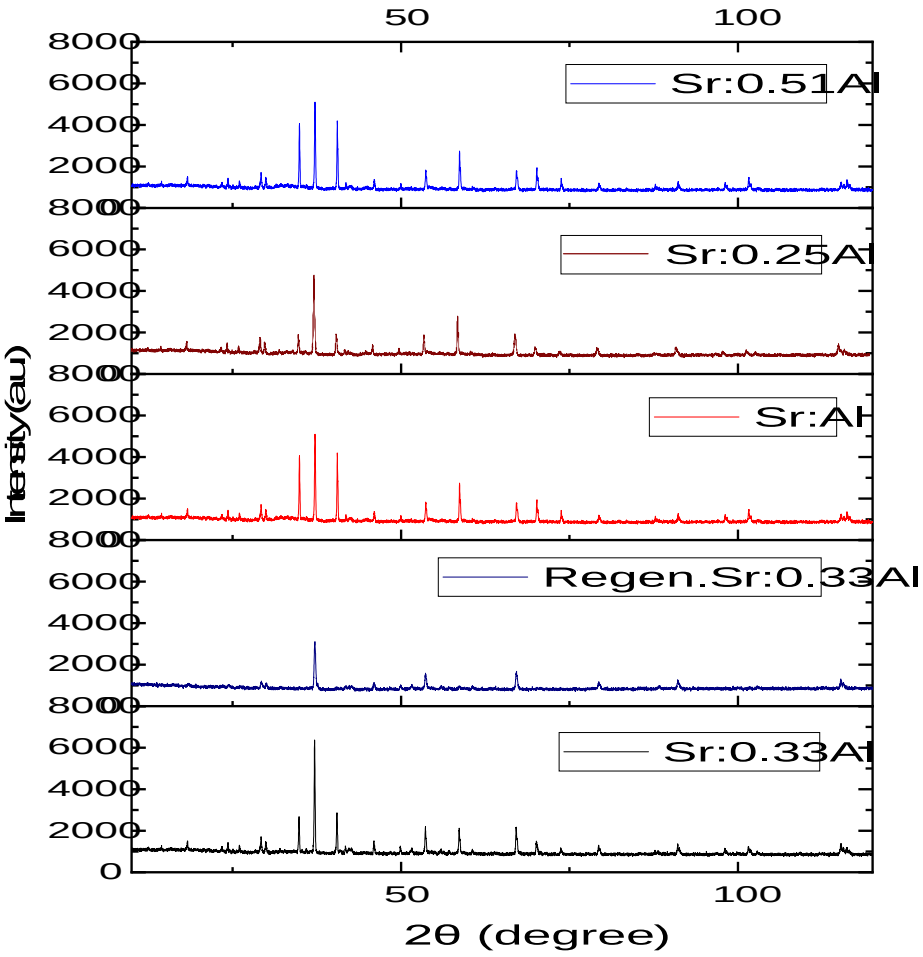

Fig. 2. XRD pattern of Sr: Al double oxides and regenerated Sr: 0.33Al

The SEM images of Sr: 0.33Al and regenerated Sr: 0.33Al are shown in Fig. 3, which provide information about the surface structure of the nanocatalyst and the morphological alterations which occurred to the catalyst after biodiesel production. The SEM image of Sr: 0.33Al shows more similar morphology of particles throughout the image with slight agglomeration. The minor distortion in the Sr: 0.33Al morphology of the catalyst is directly visible from the SEM images. The EDS graph of Sr: 0.33Al and regenerated Sr: 0.33Al shows the elemental composition of the catalyst before and after the reaction, respectively. The minor variation in the composition of catalyst possibly due to slight leaching of Sr and Al ions after regeneration and reuse of catalyst.

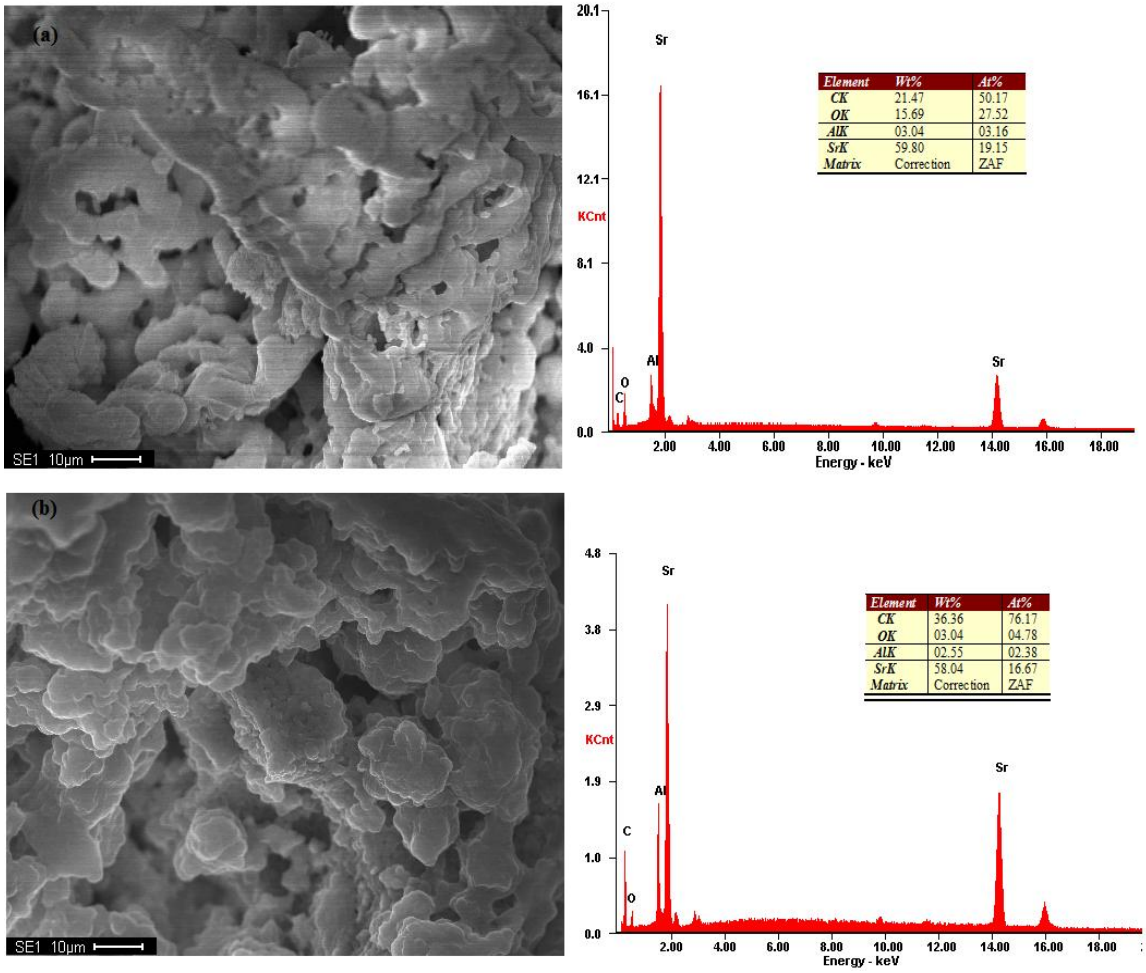

Fig 3. (a) SEM image and EDS of Sr: 0.33Al (b) SEM image and EDS of regenerated Sr: 0.33Al

The TEM image of Sr: 0.33Al and regenerated Sr: 0.33Al were depicted in Fig. 4a and 4b, respectively. The TEM images are strong agreement with the SEM results. The Sr: 0.33Al and regenerated Sr: 0.33Al catalyst have a particle size of 57-100 nm, which was confirmed with help of TEM images. The slight variation in particle form of Sr: 0.33Al and regenerated Sr: 0.33Al were also visible in TEM images.

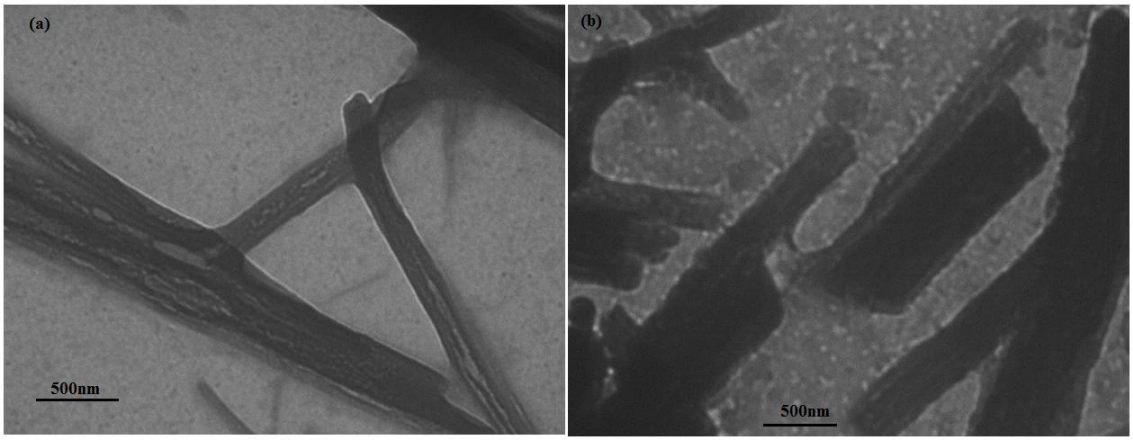

Fig. 4. TEM image of (a) Sr: 0.33Al and (b) Regenerated Sr: 0.33Al

The specific surface area, pore volume and pore size of Sr: 0.33Al and regenerated Sr: 0.33Al were summarised in Table 2. The BET surface area and average adsorption pore width and pore volume were reduced after the reaction procedure. This result explains one of the reasons for the slight reduction in catalytic activity of the regenerated Sr: 0.33Al. The N_2 adsorption-desorption isotherm for Sr: 0.33Al and regenerated Sr: 0.33Al from BET analysis is shown in Fig.5. The hysteresis loop of isotherm indicates the presence of mesoporous materials.

Table 2.

The results of Brunauer-Emmett-Teller surface area analysis

	Parameters	Sr: 0.33Al	Regenerated Sr: 0.33Al
Surface area	BET surface area (m^2/g)	0.95	0.50
	BJH adsorption cumulative surface area of pores (m^2/g)	0.49	0.20
	BJH desorption cumulative surface area of pores (m^2/g)	0.60	0.26

Pore volume	Single point adsorption total pore volume of pores (cm^3/g)	0.002	0.0009
	BJH adsorption cumulative volume of pores (cm^3/g)	0.0052	0.0027
	BJH desorption cumulative volume of pores (cm^3/g)	0,0056	0.0030
Pore size	Adsorption average pore width (nm)	8.5	6.2
	BJH adsorption average pore diameter (nm)	43.1	53.2
	BJH desorption average pore diameter (nm)	37.1	44.8

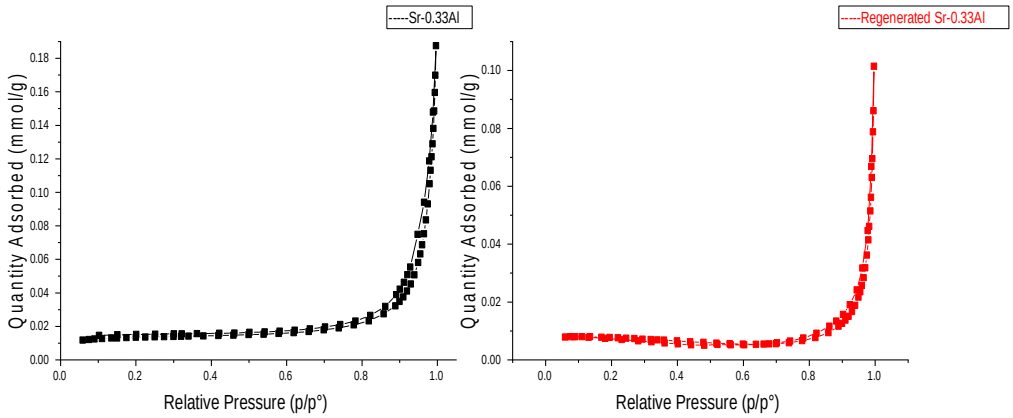

Fig. 5. N_2 adsorption-desorption isotherm plot of Sr: 0.33Al and regenerated Sr: 0.33Al

XPS was applied to examine the surface properties and binding energies (BE) of elements in Sr-Al double oxides. The chemical environment of Sr, Al, O, C were simulated by Gaussian curve-fitting of the Sr 3d, Al 2p, O 1s and C 1s spectra. Fig. 6 (a) and (b) depicts XPS fitted spectra of Sr: 0.33Al and the regenerated Sr: 0.33Al nanocatalyst. The Sr-Al double oxides depicts Sr3d signals with two peaks at binding energies of 133.1 and 134.9 eV assigned to Sr $3d_{5/2}$ and $3d_{3/2,}$ respectively[17]. The Al 2p spectra of Sr: 0.33Al and regenerated Sr: 0.33Al shows binding energy at 73 eV, which corresponds to pure Al. The pure Al helps in the formation of defective oxides that helps in trapping charges [18]. The presence of weakly adsorbed oxygen, stronger binding with adsorbed oxygen and aluminium atoms was described by a signal at 531 eV represented in O 1s spectra of Sr: 0.33Al and regenerated Sr: 0.33Al correspondingly [19]. The binding energies at 284.6 eV and 289eV in C 1s core level spectrum of Sr: 0.33Al consigned to C–C, C=O respectively. Furthermore, the C 1s spectra of regenerated Sr: 0.33Al indicates only the presence of C-C binding energies [20, 21].

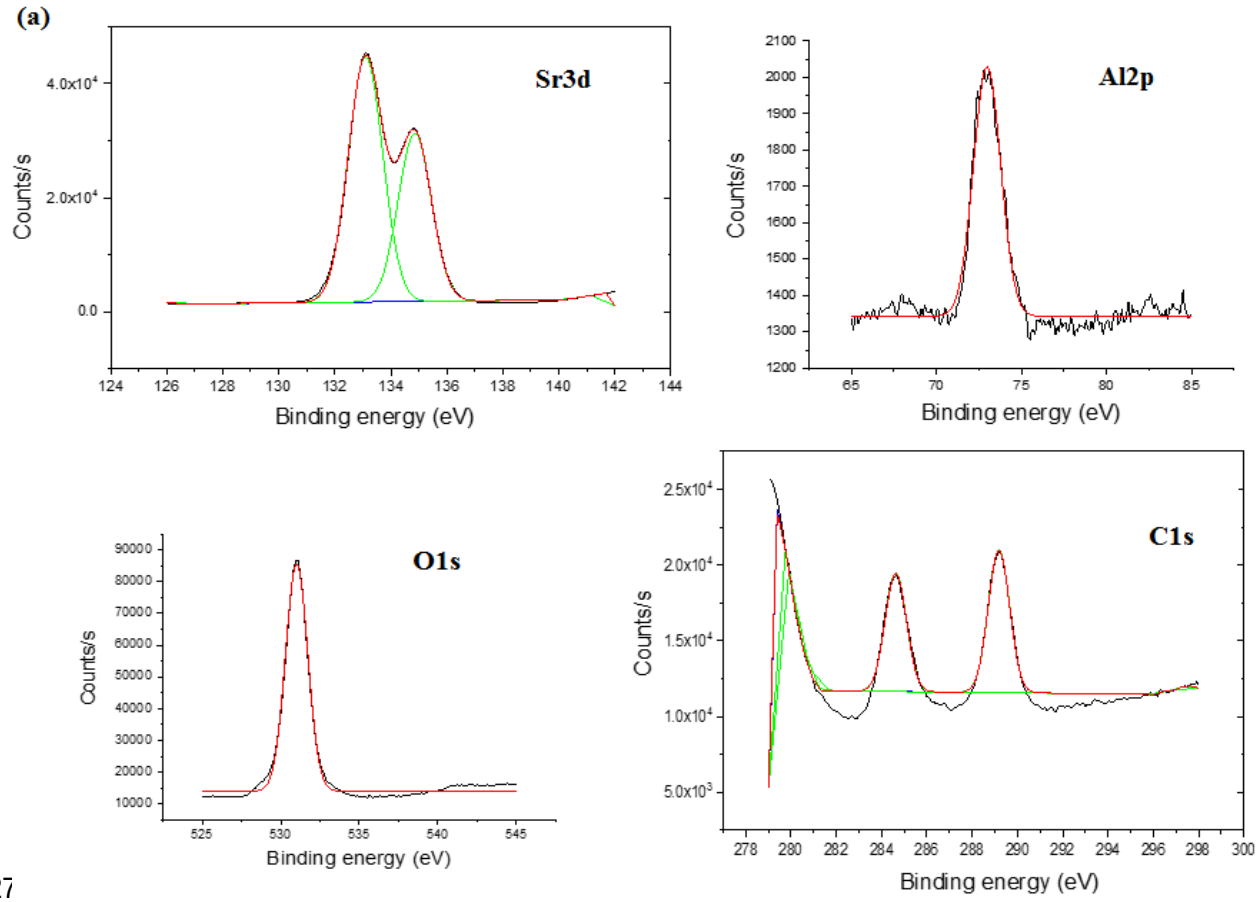
(a)
Sr3d
Counts/s
Binding energy (eV)
Al2p
Counts/s
Binding energy (eV)
O1s
Counts/s
Binding energy (eV)
C1s
Counts/s
Binding energy (eV)

27

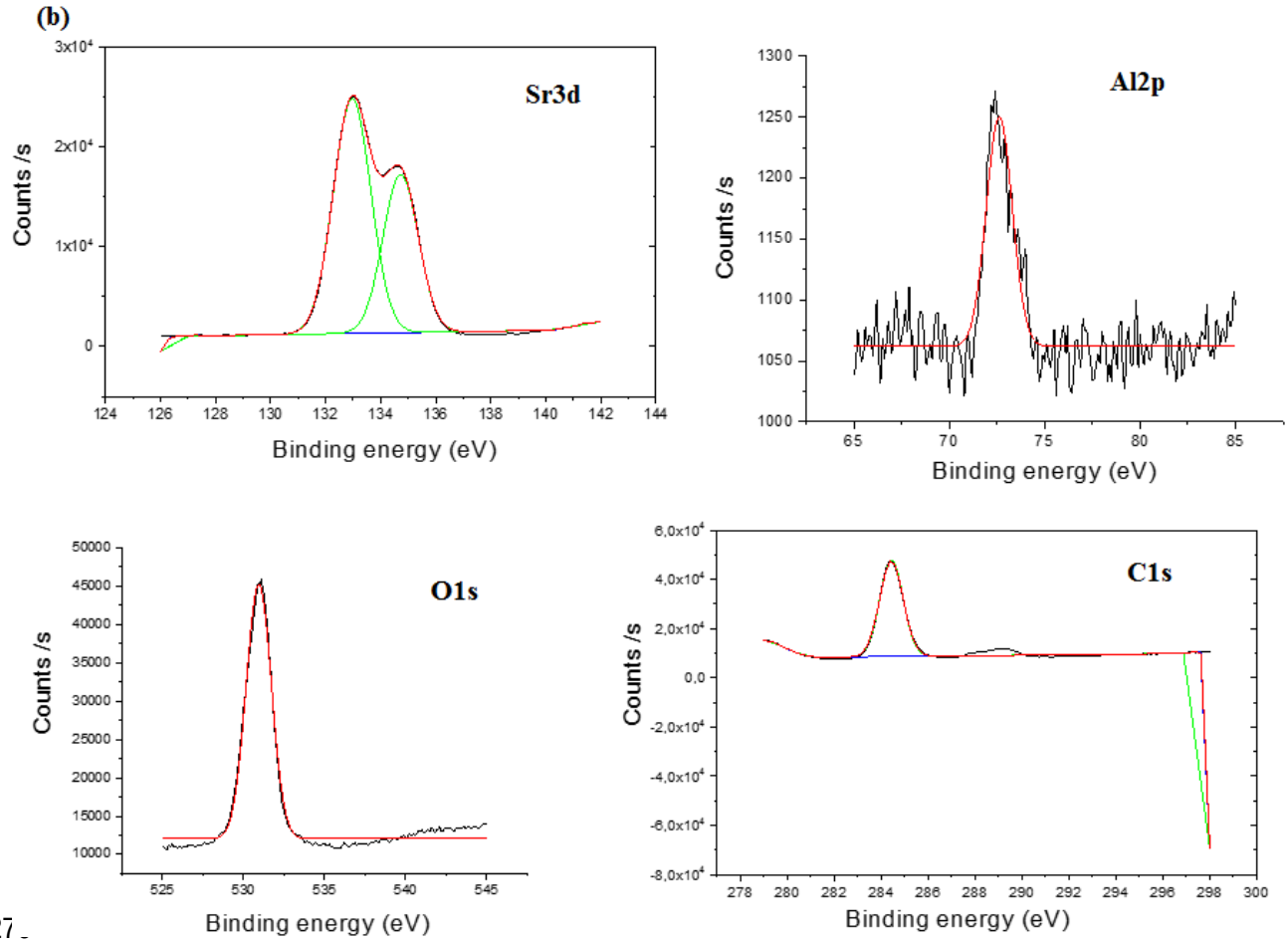

Fig. 6. XPS spectra of (a) bare Sr: 0.33Al and (b) regenerated Sr: 0.33Al nanocatalyst

3.3.Characterisation of biodiesel

The fatty acid methyl esters made from the lard oil and WCO were characterised by GC-MS, ^{1}H NMR and ^{13}C NMR. The quality of the produced biodiesel should satisfy the criteria determined by ASTM/EN 14214 limits.

The chemical composition of biodiesel was demonstrated with the help of GC-MS chromatogram and National Institute of Standards and Technology (NIST) 2014 MS library. The fatty acid methyl esters obtained after the transesterification of lard oil and waste cooking oil with Sr: 0.33Al illustrated in Fig 7. Each FAME peak in the sample

was recognised with the help of a library match and the obtained outcomes were represented in Table 3.

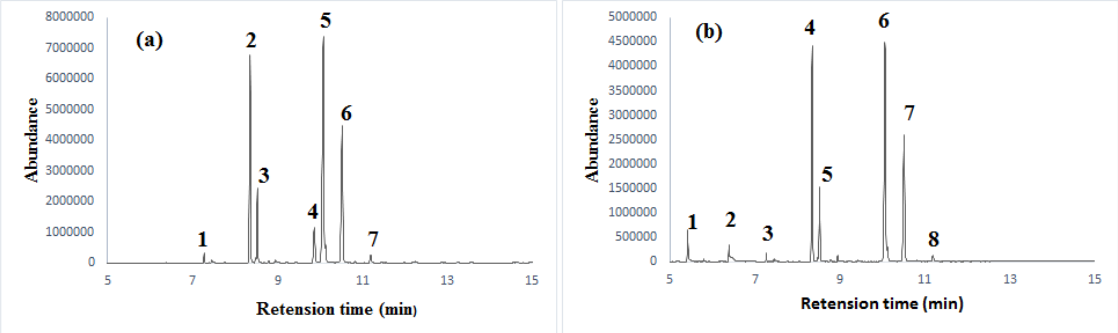

Fig. 7. Illustrates the GC-MS spectrum of biodiesel obtained from (a) lard oil and (b) waste cooking oil, after transesterification with 0.6 wt Sr: 0.33Al , 1:4.5 oil to the methanol molar ratio at 40°C for 30 min.

Table 3.

The composition of biodiesel obtained after transesterification with Sr: 0.33Al.

Peak	**Lard oil FAME**		**Compound name**
	Retention time (min)	Library match (%)	
1	7.3	92.6	methyl 12-methyltridecanoate
2	8.4	91.5	methyl hexadecanoate
3	8.5	94.4	methyl (Z)-hexadec-9-enoate
4	9.9	93.5	methyl octadecanoate
5	10.1	96	methyl (E)-octadec-13-enoate
6	10.5	96.5	methyl (11E,14E)-octadeca-11,14-dienoate

7	11.2	89	methyl (9Z,12Z,15Z)-octadeca-9,12,15-trienoate

	Waste cooking oil FAME		Compound name
	Retention time (min)	Library match (%)	
1	5.4	89.9	methyl decanoate
2	6.4	84.6	methyl dodecanoate
3	7.3	92.9	methyl 12-methyltridecanoate
4	8.4	90.3	methyl hexadecanoate
5	8.8	85	methyl 14-methylpentadecanoate
6	10.1	96.8	methyl (E)-octadec-13-enoate
7	10.5	96.4	methyl (11E,14E)-octadeca-11,14-dienoate
8	11.2	93.2	methyl (9Z,12Z,15Z)-octadeca-9,12,15-trienoate

The yield of fatty acid methyl esters derived from lard and waste cooking oil was estimated using ^{1}H and ^{13}C NMR spectroscopy. The conversion was calculated using equation 2, which was already mentioned hereinabove. With the help of ^{1}H NMR, FAME percentage of sample obtained after transesterification of lard oil and waste cooking oil with Sr: 0.33Al was found to be 99.7% and 99.4% correspondingly. Fig. 8a and 8b demonstrates the ^{1}H NMR spectrum of fatty acid methyl esters sample obtained from lard and waste cooking oil with help of Sr: 0.33Al as catalyst, respectively. It helps to characterise FAME and can be used to conform the existence of methyl esters in the biodiesel.

In ^{1}H NMR, the signal at 3.63 ppm indicates methoxy group (A_{ME}) of FAME and signal at 2.27 ppm corresponding to the methylene group (A_{CH2}). The presence of these signal in the biodiesel sample verifies the presence of methyl ester. Apart from the signal used for the quantification, there are other identifiable peaks such as the signal at 0.83 to

0.86 ppm for CH_2-CH_3 or for latter methyl group. The peaks in the range of 1.22 to 2.3 represents CH_2 (methylene group). The signals at 5.3 range indicates the presence of CH=CH (double bond) groups or olefinic groups [22, 23] The 3.45ppm corresponds to solvent residual signal[42]. Fig S1 (a) and S1 (b) represents ^{13}C NMR spectra of biodiesel obtained after transesterification of lard and waste oil with Sr: 0.33Al as nanocatalyst. In ^{13}C NMR, the signal in the range of 174 ppm and 51 ppm indicates the existence of ester carbonyl –COO- and C-O, respectively. The unsaturation in biodiesel sample was confirmed with help of signals over the ppm range 126-132 ppm. The presence of the -CH_2 group was shown with the help of the signals in the region of 21-35 ppm [23]The peaks 0-55 ppm corresponds to aliphatic carbon in fatty acid esters [43,44].

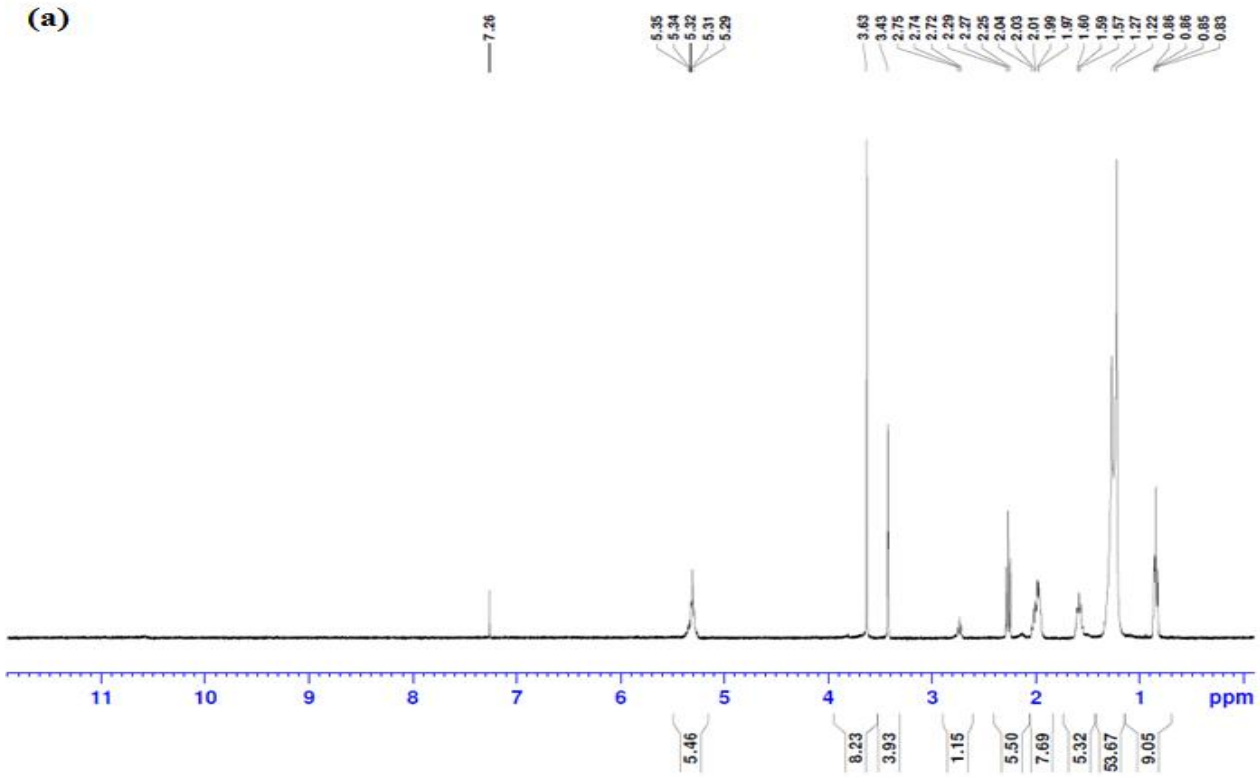

Fig. 8 a. The ^{1}H NMR for the biodiesel sample obtained from lard oil with Sr: 0.33Al

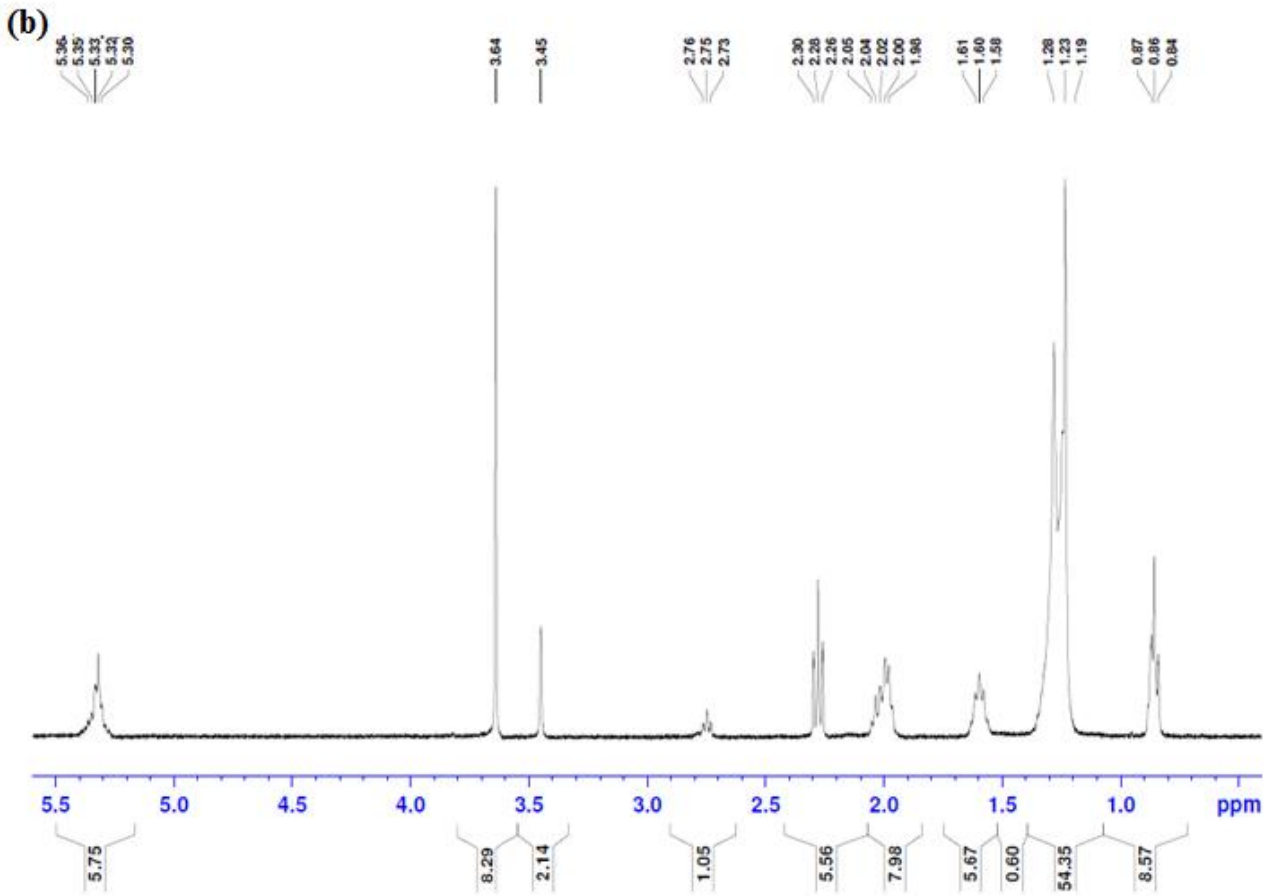

Fig. 8 b. The ^{1}H NMR for the biodiesel sample obtained from waste cooking oil with Sr: 0.33Al

3.4. Influence of various parameters on biodiesel production

The higher yield of biodiesel was achieved by optimising the reaction conditions such as the amount of co-solvent, oil to methanol ratio, reaction temperature, reaction time and catalyst amount. Based on the preliminary screening of catalysts, the Sr: 0.33Al catalyst was found to be a more capable catalyst for the conversion of lard and waste cooking oil to biodiesel. A series of transesterification reactions were performed using Sr: 0.33Al and optimised in order to achieve the reaction parameters for optimisation.

3.4.1 Effect of various co-solvents on biodiesel production

Fig 9. (a) shows the influence of various co-solvent on biodiesel production from different oils. The quantity of co-solvent varied over the range of 5-20 wt% based on the weight of oil used for the transesterification reaction. Based on reported studies co-solvent enhance interaction between reactants in presence of minimum amount of catalyst and oil to methanol ratio[8-10]. Therefore slightly higher theoretical minimum of oil to methanol ratio is used to determine effect of co-solvent on transesterification reaction. The evaluation of the effect of the co-solvent on the biodiesel production procedure was attained by performing the transesterification of each oil at 40°C by using 0.6 wt% catalyst and 1:3.5 oil to the methanol molar ratio for 40 min in the presence of various weight percentage of acetone and THF, respectively. Generally, the co-solvent helps to increase the miscibility of reactants in a transesterification reaction and thereby results in a higher yield of fatty acid methyl esters. On the contrary, a larger amount of co-solvent above the optimum value hinders the phase separation of biodiesel and glycerol [8-10]. In the present study, it was observed that the samples with 5 wt% of THF resulted in the maximum yield of FAME from both lard and waste cooking oil. This can be interpreted to means 5 wt% of THF is enough and efficient to enhance the following factors such as the solubility of methanol and oil, phase separation of FAME and glycerol and for separation of glycerol from reaction mixture.

3.4.2 Effect of temperature on biodiesel production

The influence of temperature on transesterification reaction was investigated by conducting a reaction at various temperatures using 0.9 wt% catalyst, 5 wt% THF, 1:5.5 oil to methanol molar ratio for 45 min reaction time (Fig. 9b). The temperature range chosen for the reaction was lower than the boiling point of THF. The yield of biodiesel from lard oil and WCO increased gradually up to 99.7% and 99.4% at 50°C and 60°C, respectively, and resulted in the maximum yield of fatty acid methyl esters. Moreover, the temperature has a direct effect on the rate of the reaction but elevation in temperature

after the optimum value decreases the yield of biodiesel which is due to the fact that an elevated temperature favours methanol or co-solvent vaporisation [10, 24, 25]. Further experiments were conducted at 50°C and 60°C for lard and WCO, respectively.

3.4.3 Effect of the reaction time on biodiesel production

The effect of the reaction time on the transesterification reaction of lard oil and WCO was observed by executing reactions for various time intervals using 0.9 wt% catalyst, 1:5.5 oil to methanol molar ratio at 50°C and 60°C correspondingly were depicted in Fig. 9c. The present investigation was employed to represent the effect of THF on the rate of the transesterification reaction. The fatty acid methyl ester content rose with the increase in reaction time and reached its maximum with a shorter interval of time in the reaction mixtures with the co-solvent. This is due to the reduction of the phase boundary in reactants and a faster separation of biodiesel and glycerol.

3.4.4 Effect of the catalyst amount (weight%) in biodiesel production

Fig 9d was applied to determine the effect of the catalyst concentration on biodiesel production by performing reactions at various catalyst concentration from 0.2% to 1.2 wt% of oil. The 99.7% and 99.4% of biodiesel yield was obtained from lard oil and waste cooking oil using 0.9 wt% catalyst, 5 wt% THF as the co-solvent and 1:5.5 oil to methanol molar ratio within 45 min of the reaction time at 50°C and 60°C correspondingly. The conversion of oil to biodiesel raises with an increase in the amount of catalyst up to 0.9 wt% and extra rise in the catalyst concentration beyond the optimum value showed reduction in biodiesel yield due to a decrease in the availability of active sites and hindrance to phase separation [9, 26, 27].

3.4.5 Effect of oil to methanol ratio in biodiesel production

The biodiesel conversion significantly increases as oil to methanol molar ratios were raised from 1:3.5 to 1:6.5 as illustrated in Fig. 9e. The lard oil and waste cooking oil

transesterification process was carried out with 0.9 wt% catalyst for 45 min of reaction time at 50°C and 60°C, respectively. The biodiesel yield was negatively affected by a rising methanol concentration above the optimum amount (1:5.5) which was due to the higher solubility of glycerol to ester phase resulting in difficulty for the separation of biodiesel. It may also support a reverse reaction than the production of biodiesel [28, 29].

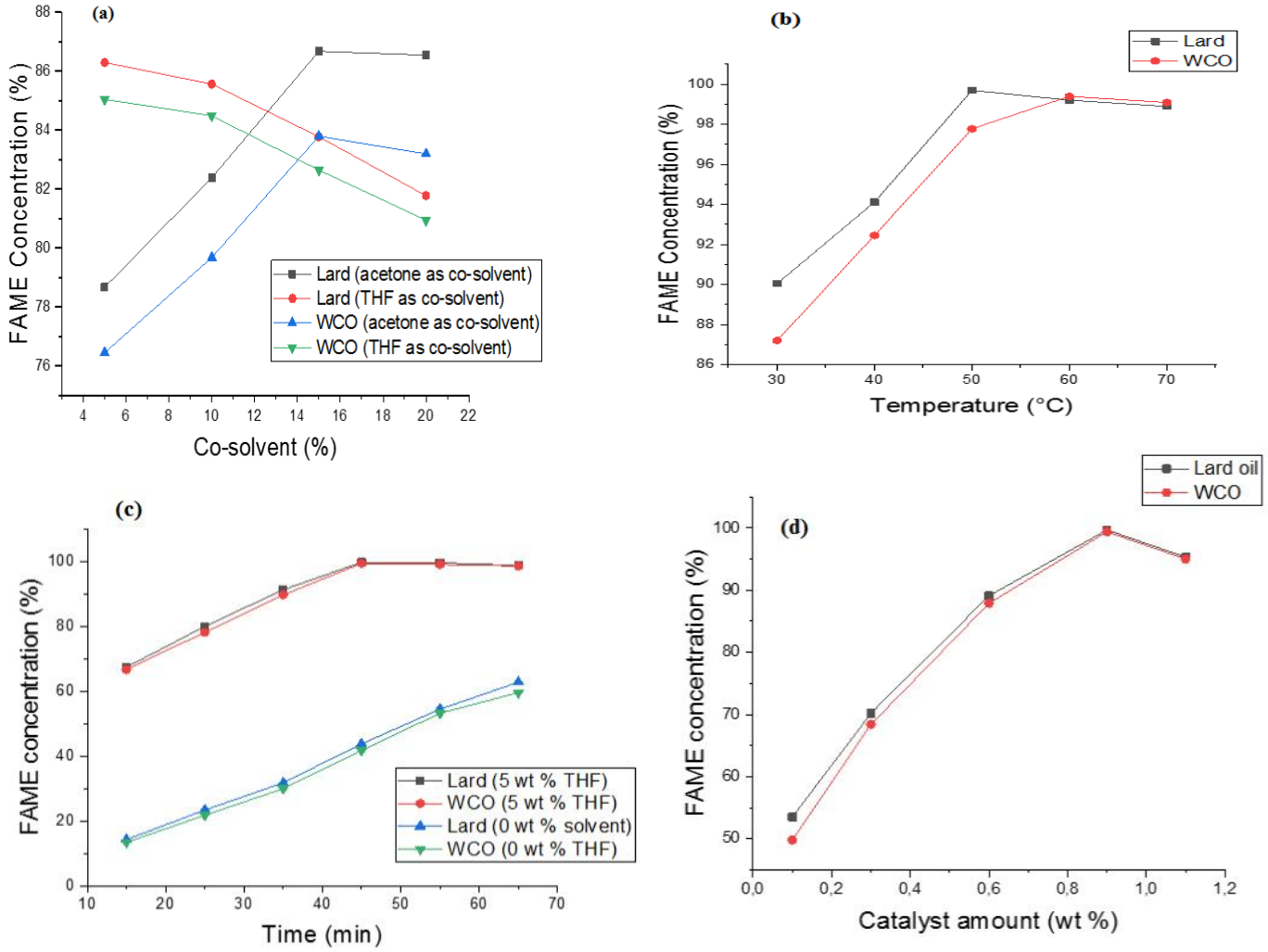

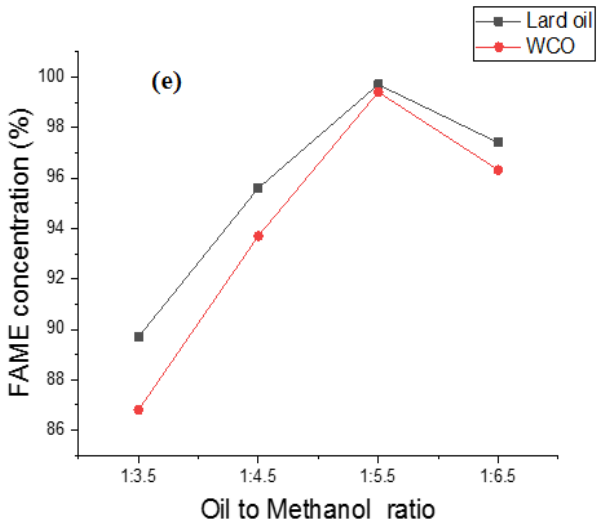

Fig. 9. (a). Effect of various co-solvents on the biodiesel yield (b). Effect of the reaction temperature on the biodiesel yield (c). Effect of the reaction time on the biodiesel yield (d) Effect of the catalyst amount (weight %) on the biodiesel yield (e) Effect of the oil to methanol molar ratio on the biodiesel yield.

3.5. Properties of synthesised biodiesel

The properties of fatty acid methyl esters were determined using the EN 14214/ASTM D6751 method as shown in Table 4. All of these features play a key role in the biodiesel quality. The acid value of lard oil methyl ester and WCO methyl ester were found to be 0.29 mg KOH/g and 0.31 mg KOH/g, respectively. The resulted acid values were within the limits of the European International standard organisation (EN ISO) method. The increase in acid value can result in difficulties like corrosion of rubber parts of engine and filter clogging [30]. The density and kinematic viscosity are other two main fuel features that influence the fuel injection operation. Higher values of these factors can negatively affect the fuel injection process and leads in the formation of engine deposits [31, 32]. The density and kinematic viscosity of both methyl esters were within EN ISO 12185 and EN ISO 3104 limits correspondingly. The other factor is flash point, which specifies the minimum temperature at which fuel starts to ignite. It is vital to know the flash point value for fuel handling and storage [33]. Cloud point is important when fuel is exposed to lower

temperature where as cetane number directly connects to quality of fuel. The rest of the preferred features such as calorific value, cloud point, cetane number, and pour point are also within EN ISO/ASTM limits.

Table 4.

Properties of fatty acid methyl esters from different feedstocks

Property	EN 14214/ ASTM D6751 test method	Limits	Methyl ester from Lard oil	Methyl ester from WCO
Acid value (mg KOH/g)	Pr EN14104	0.5 max	0.29	0.31
Density at 15°C (kg/m^3)	EN ISO 12185	860-900	882.1	885.6
Kinematic viscosity at 40°C mm^2/s	EN ISO 3104	3-5	3.98	4.01
Calorific value (MJ/kg)	D6751		39.92	40.45
Flash point (°C)	EN ISO 2719	-	131°C	138°C
Cetane number	EN ISO 5165	≥51	63	67
Cloud point (°C)	D2500		8	9
Pour point (°C)	ISO 3016		5	7

3.6. Reusability of catalyst

The concept of catalyst reusability plays a vital role in an environmentally friendly biodiesel production process. Therefore, the catalyst recovered after the transesterification reaction was subjected to a cleaning process to remove the deposited oil, products or glycerol. The cleaning of the catalyst with a suitable solvent and calcination helps in its regeneration [11,34]. The catalytic reusability of the Sr-0.25Al nanocatalyst was analysed by the separation of the catalyst from fatty acid methyl esters

and glycerol. The catalytic reusability Sr: 0.33Al over lard oil and waste cooking oil using 0.9 wt% catalyst, 5 wt% THF as co-solvent and 1:5.5 oil to methanol molar ratio within 45 min of reaction time at 50°C and 60°C correspondingly depicted in Fig. 10. Lard oil and WCO biodiesel yields were decreased from 99.7% to 95.1% and 99.4% to 93.7%, respectively, in four cycles. Compared to other reported studies the current catalyst showed higher stability and better biodiesel yield even after five cycles of reaction[11,26, 38,39,40]. The minor changes in the catalyst structure and composition, reduction in BET surface area illustrated in catalyst characterisation findings agrees with the drop in catalytic activity. The reusability test showed that the regenerated catalyst was quite efficient even after four cycles with the significant conversion of oil into biodiesel. The nanocatalyst stability after various cycles were evaluated based on the the leached metal ion concentration. The Agilent 5110 Inductively coupled plasma (ICP) was used to measure metal concentration. It was detected that from cycle 1 to cycle 5, the Al and Sr concentrations in solution were less than 0.0072 and 0.024mg/L.

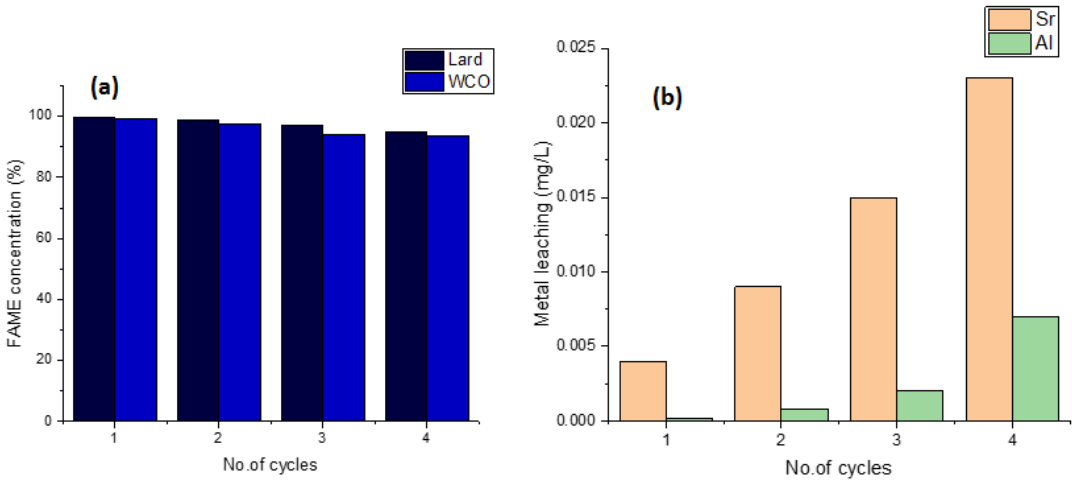

Fig. 10. (a) Reusability analysis of Sr: 0.33Al catalyst and (b) Stability of Sr: 0.33Al catalyst up to four transesterification reactions

4. **Conclusion**

The Sr-Al doubleoxides were synthesised and employed for the transesterification reaction of lard and waste cooking oil to biodiesel. The influence of acetone and THF as a co-solvent on biodiesel production were investigated. The combined effect of a co-solvent and nanocatalyst on lard and waste cooking oil were examined. The best catalytic activity was attained with Sr: 0.33Al as a nanocatalyst and THF as a co-solvent. The characterisation of synthesised catalyst and regenerated catalyst were performed by FTIR, XRD, SEM, TEM, XPS and BET. It helps to determine the morphology, composition and stability of the catalyst before and after the transesterification reaction. The factors affecting biodiesel production were optimised. The maximum yield of 99.7% and 99.4% of lard oil methyl ester and WCO biodiesel was observed with 5 wt% THF, 0.9 wt% catalyst amount, 1:5.5 oil to methanol ratio with in a reaction time of 45 minutes at 50°C and 60°C, respectively. The presence of the co-solvent increases the reaction rate and reduction in methanol consumption compared to the usual transesterification reaction. The reusability of the catalyst also exhibited a favourable result, which makes it cost effective and eco-friendlier. The properties of biodiesel such as acid value, density, kinematic viscosity and flash point were within the EN 14214 limits. All these results summarise the efficiency of Sr-Al nanocatalysts as a potential catalyst and THF as a better co-solvent for the production of superior quality biodiesel from different feedstock.

References

[1] J. Hossain, Bio-Diesel from Mustard Oil: A Renewable Alternative Fuel for Small Diesel Engines, Mod. Mech. Eng. 1 (2011) 77–83. doi:10.4236/mme.2011.12010.

[2] L. Wen, Y. Wang, D. Lu, S. Hu, H. Han, Preparation of KF/CaO nanocatalyst and its application in biodiesel production from Chinese tallow seed oil, Fuel. 89 (2010) 2267–2271. doi:10.1016/j.fuel.2010.01.028.

[3] W. Roschat, T. Siritanon, T. Kaewpuang, B. Yoosuk, Economical and green biodiesel production process using river snail shells-derived heterogeneous catalyst and co-solvent method, Bioresour. Technol. 209 (2016) 343–350. doi:10.1016/j.biortech.2016.03.038.

[4] I. Thushari, S. Babel, Bioresource Technology Sustainable utilization of waste palm oil and sulfonated carbon catalyst derived from coconut meal residue for biodiesel production, Bioresour. Technol. 248 (2018) 199–203.

527 doi:10.1016/j.biortech.2017.06.106.
528 [5] G. Baskar, I.A.E. Selvakumari, R. Aiswarya, Biodiesel production from castor oil
529 using heterogeneous Ni doped ZnO nanocatalyst, Bioresour. Technol. 250 (2018)
530 793–798. doi:10.1016/j.biortech.2017.12.010.
531 [6] L.T. Thanh, K. Okitsu, L. Van Boi, Y. Maeda, Catalytic Technologies for
532 Biodiesel Fuel Production and Utilization of Glycerol: A Review, Catalysts. 2
533 (2012) 191–222. doi:10.3390/catal2010191.
534 [7] S.P. Singh, D. Singh, Biodiesel production through the use of different sources and
535 characterization of oils and their esters as the substitute of diesel: A review, Renew.
536 Sustain. Energy Rev. 14 (2010) 200–216. doi:10.1016/j.rser.2009.07.017.
537 [8] L. Tu, K. Okitsu, Y. Sadanaga, N. Takenaka, Y. Maeda, A new co-solvent method
538 for the green production of biodiesel fuel – Optimization and practical application,
539 Fuel. 103 (2013) 742–748. doi:10.1016/j.fuel.2012.09.029.
540 [9] J.M. Encinar, A. Pardal, N. Sánchez, An improvement to the transesterification
541 process by the use of co-solvents to produce biodiesel, Fuel.166 (2016) 51–58.
542 [10] V. Singh, M. Yadav, Y.C. Sharma, Effect of co-solvent on biodiesel production
543 using calcium aluminium oxide as a reusable catalyst and waste vegetable oil, Fuel.
544 203 (2017) 360–369. doi:10.1016/j.fuel.2017.04.111.
545 [11] I. Ambat, V. Srivastava, M. Sillanpää, Recent advancement in biodiesel production
546 methodologies using various feedstock : A review, Renewable and Sustainable
547 Energy Reviews . 90 (2018) 356–369.
548 [12] S. Sakthivel, S. Halder, P.D. Gupta, Influence of Co-Solvent on the Production of
549 Biodiesel in Batch and Continuous Process, International Journal of Green Energy.
550 10 (2013) 876-884. doi:10.1080/15435075.2012.727365.
551 [13] M. Feyzi, N. Hosseini, N. Yaghobi, R. Ezzati, Preparation, characterization, kinetic
552 and thermodynamic studies of MgO-La_2O_3 nanocatalysts for biodiesel production
553 from sunflower oil, Chem. Phys. Lett. 677 (2017) 19–29.
554 doi:10.1016/j.cplett.2017.03.014.
555 [14] M. Saniger, Al-0 infrared vibrational frequencies of y-alumina, Materials Letters.
556 22 (1995) 109–113.
557 [15] L. Song, Y. Li, P. He, S. Zhang, X. Wu, S. Fang, J. Shan, D. Sun, Ultrasonics
558 Sonochemistry Synthesis and sonocatalytic property of rod-shape $Sr(OH)_2.8H_2O$,

559 Ultrasonics Sonochemistry.21 (2014) 1318–1324.
560 [16] E. Rashtizadeh, F. Farzaneh, Z. Talebpour, Synthesis and characterization of
561 $Sr_3Al_2O_6$ nanocomposite as catalyst for biodiesel production, Bioresour. Technol.
562 154 (2014) 32–37. doi:10.1016/j.biortech.2013.12.014.
563 [17] W. Chen, Q. Liu, One-step in situ synthesis of strontium ferrites and strontium
564 ferrites / graphene composites as microwave absorbing materials , RSC Advances.
565 (2017) 40650–40657. doi:10.1039/c7ra05700h.
566 [18] H. Kang, M.S.P. Reddy, D. Kim, Effect of oxygen species on the positive flat-band
567 voltage shift in Al_2O_3 / GaN metal – insulator – semiconductor capacitors with
568 post-deposition annealing, J. Phys. D: Appl. Phys. 46 (2013). doi:10.1088/0022-
569 3727/46/15/155101.
570 [19] C. Maldonado, C.J. Lucio-ortiz, Low Concentration Fe-Doped Alumina Catalysts
571 Using Sol-Gel and Impregnation Methods: The Synthesis, Characterization and
572 Catalytic Performance during the Combustion of Trichloroethylene, Materials.
573 (2014) 2062-2086. doi:10.3390/ma7032062.
574 [20] M. Wang, J. Han, Y. Hu, R. Guo, Mesoporous C, N-codoped TiO_2 hybrid shells
575 withenhanced visible light photocatalytic performance, RSC Adv. 7 (2017) 15513–
576 15520. doi:10.1039/C7RA00985B.
577 [21] S.S. Pitale, I.M. Nagpure, V. Kumar, O.M. Ntwaeaborwa, J.J. Terblans, H.C.
578 Swart, Investigations on the low voltage cathodoluminescence stability and surface
579 chemical behaviour using Auger and X-ray photoelectron spectroscopy on, Mater.
580 Res. Bull. 46 (2011) 987–994. doi:10.1016/j.materresbull.2011.03.022.
581 [22] M. Tariq, S. Ali, F. Ahmad, M. Ahmad, M. Zafar, N. Khalid, M.A. Khan,
582 Identification, FT-IR, NMR (^{1}H and ^{13}C) and GC/MS studies of fatty acid methyl
583 esters in biodiesel from rocket seed oil, Fuel Process. Technol. 92 (2011) 336–341.
584 doi:10.1016/j.fuproc.2010.09.025.
585 [23] M. Tariq, S. Ali, N. Khalid, Activity of homogeneous and heterogeneous catalysts,
586 spectroscopic and chromatographic characterization of biodiesel: A review,
587 Renew. Sustain. Energy Rev. 16 (2012) 6303–6316.
588 doi:10.1016/j.rser.2012.07.005.
589 [24] E.C. Abbah, G.I. Nwandikom, C.C. Egwuonwu, N.R. Nwakuba, Effect of Reaction
590 Temperature on the Yield of Biodiesel From Neem Seed Oil, Am. J. Energy Sci. 3

591 (2016) 16–20.
592 [25] T. Eevera, K. Rajendran, S. Saradha, Biodiesel production process optimization
593 and characterization to assess the suitability of the product for varied
594 environmental conditions, Renew. Energy. 34 (2009) 762–765.
595 doi:10.1016/j.renene.2008.04.006.
596 [26] V. Singh, F. Bux, Y.C. Sharma, A low cost one pot synthesis of biodiesel from
597 waste frying oil (WFO) using a novel material, β-potassium dizirconate (β-
598 $K_2Zr_2O_5$), Appl. Energy. (2016). doi:10.1016/j.apenergy.2016.02.135.
599 [27] M. Takase, Y. Chen, H. Liu, T. Zhao, L. Yang, X. Wu, Biodiesel production from
600 non-edible Silybum marianum oil using heterogeneous solid base catalyst under
601 ultrasonication, Ultrason. Sonochem. 21 (2014) 1752–1762.
602 doi:10.1016/j.ultsonch.2014.04.003.
603 [28] G. Kafui, A. Sunnu, J. Parbey, Effect of biodiesel production parameters on
604 viscosity and yield of methyl esters : Jatropha curcas , Elaeis guineensis and Cocos
605 nucifera, Alexandria Eng. J. 54 (2015) 1285–1290. doi:10.1016/j.aej.2015.09.011.
606 [29] F.F. Banihani, Transesterification and Production of Biodiesel from Waste
607 Cooking Oil : Effect of Operation Variables on Fuel Properties, American Journal
608 of Chemical Engineering . 4 (2017) 154–160. doi:10.11648/j.ajche.20160406.13.
609 [30] A.B. Chhetri, K.C. Watts, M.R. Islam, Waste Cooking Oil as an Alternate
610 Feedstock for Biodiesel Production, Energies. 1 (2008) 3–18.
611 doi:10.3390/en1010003.
612 [31] G. Knothe, K.R. Steidley, Kinematic viscosity of biodiesel fuel components and
613 related compounds. Influence of compound structure and comparison to
614 petrodiesel fuel components, Fuel. 84 (2005) 1059–1065.
615 doi:10.1016/j.fuel.2005.01.016.
616 [32] A. Demirbas, Biodiesel: A realistic fuel alternative for diesel engines, Biodiesel A
617 Realis. Fuel Altern. Diesel Engines. (2008) 1–208. doi:10.1007/978-1-84628-995-
618 8.
619 [33] H.G. Aleme, P.J.S. Barbeira, Determination of flash point and cetane index in
620 diesel using distillation curves and multivariate calibration, Fuel. 102 (2012) 129–
621 134. doi:10.1016/j.fuel.2012.06.015.
622 [34] W. V. Prescott, A.I. Schwartz, Nanorods and Nanomaterials Research Progress,

623 (2008) 279.
624 http://books.google.es/books/about/Nanorods_Nanotubes_and_Nanomaterials_R
625 es.html?id=a2De3CXrM8wC&pgis=1.
626 [35] Kaur N, Ali A. Lithium ions-supported magnesium oxide as nano-sized solid catalyst
627 for biodiesel preparation from mutton fat, Energy Sources, Part A Recover Util
628 Environ Eff. 35 (2013)184–192.
629 [36] Tahvildari K, Anaraki YN, Fazaeli R, Mirpanji S, Delrish E. The study of CaO and
630 MgO heterogenic nano-catalyst coupling on transesterification reaction efficacy in
631 the production of biodiesel from recycled cooking oil., Iran. J Environ Heal Sci
632 Eng 13(2015)1–9. http://dx.doi.org/10.1186/s40201-015-0226-7.
633 [37] Ambat I, Srivastava V, Haapaniemi E et al. Nano-magnetic potassium impregnated
634 ceria as catalyst for the biodiesel production , Renew Energy 139 (2019)1428–
635 1436.
636 [38] Galván G, Romero R, Ramírez A, Luz S, Baeza-jiménez R, Natividad R. Biodiesel
637 production from used cooking oil and sea sand as heterogeneous catalyst, Fuel.
638 138(2014) 143–148. doi:10.1016/j.fuel.2014.07.053.
639 [39] Berrios M, Gutiérrez MC, Martín MA, Martín A. Application of the factorial design
640 of experiments to biodiesel production from lard, Fuel Process Technol 90 (2009)
641 1447–1451. doi:10.1016/j.fuproc.2009.06.026.
642 [40] Ezekannagha CB, Ude CN, Onukwuli OD. Optimization of the methanolysis of lard
643 oil in the production of biodiesel with response surface methodology, Egypt J Pet
644 26 (2017) 1001-1011. doi:10.1016/j.ejpe.2016.12.004.
645 [41] Alonso JA, Rasines I, Soubeyroux JL. Tristrontium dialuminum hexaoxide: An
646 intricate superstructure of nanocatalyst, ChemInform. 29(1990) 4768–4771.
647 doi:10.1021/ic00348a035.
648 [42] Fulmer GR, Miller AJM, Sherden NH, Gottlieb HE, Nudelman A, Stoltz BM, et
649 al. NMR Chemical Shifts of Trace Impurities : Common Laboratory Solvents ,
650 Organics , and Gases in Deuterated Solvents Relevant to the Organometallic
651 Chemist, Organometallics. 29 (2010) 2176–2179. doi:10.1021/om100106e.
652 [43] Alexandri E, Ahmed R, Siddiqui H, Choudhary MI, Tsiafoulis CG, Gerothanassis
653 IP. High Resolution NMR Spectroscopy as a Structural and Analytical Tool for
654 Unsaturated Lipids in Solution, Molecules 22 (2017) 1–71.

655 doi:10.3390/molecules22101663.
656 [44] Piterina A V, Barlett J, Pembroke JT. C-NMR Assessment of the Pattern of Organic
657 Matter Transformation during Domestic Wastewater Treatment by Autothermal
658 Aerobic Digestion (ATAD), International Journal of Environmental Research and
659 Public Health 2009 2288–2306. doi:10.3390/ijerph6082288
660 [45] Megha U, Shijina K, Varghese G. Nanosized $LaCo_{0.6}Fe_{0.4}O_3$ perovskites
661 synthesized by citrate sol gel auto combustion method, Processing and Application
662 of Ceramics 8 (2014) 87-92. doi:10.2298/PAC1402087M.
663 [46] Xu Y, He Y, Yuan X. Preparation of nanocrystalline $Sr_3Al_2O_6$ powders via citric
664 acid precursor 2007;172:99–102. doi:10.1016/j.powtec.2006.10.045.
665
666
667
668
669
670
671
672
673
674
675
676
677
678
679
680
681
682
683
684

Effect of different co-solvents on biodiesel production from various low-cost feedstocks using Sr-Al double oxides

Indu Ambat [a]*, Varsha Srivastava [a], Sidra Iftekhar [a], Esa Haapaniemi [b], Mika Sillanpää [a]

[a] Department of Green Chemistry, School of Engineering Science, Lappeenranta University of Technology, Sammonkatu 12, FI-50130 Mikkeli, Finland

[b] Department of Organic Chemistry, University of Jyväskylä, Finland

*Corresponding Author (E-mail: indu.ambat@lut.fi)

Supplementary materials

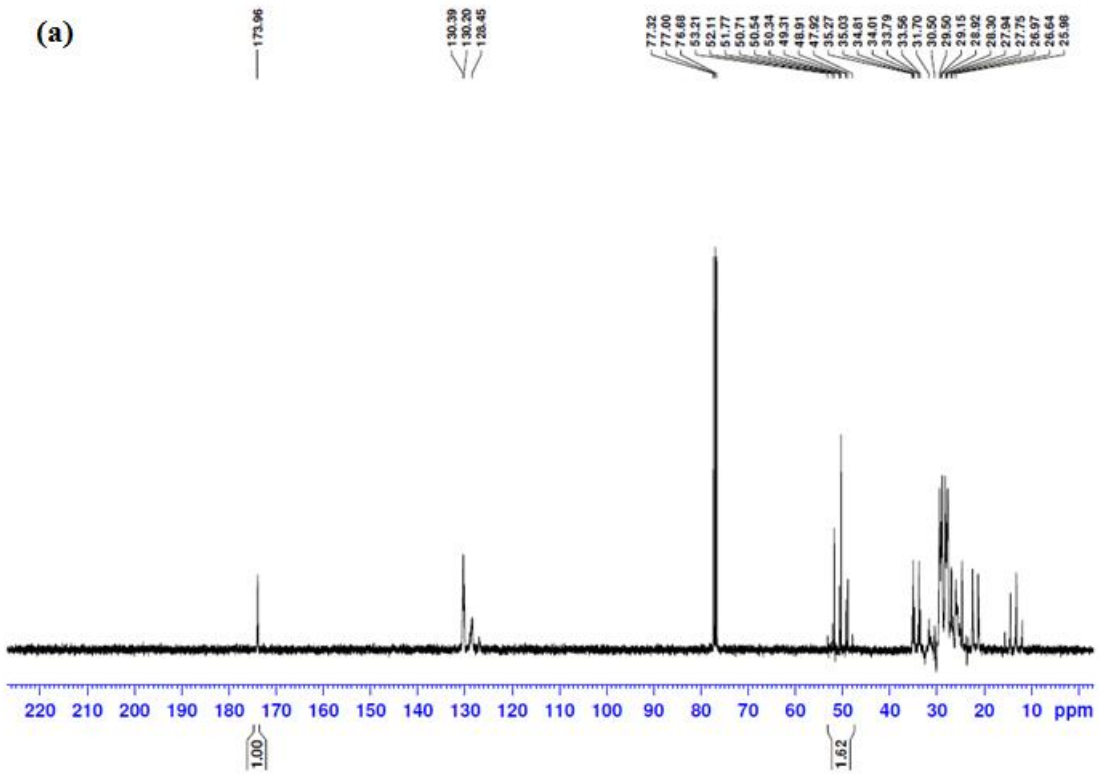

Fig S1 (a). The ^{13}C NMR for the biodiesel sample obtained from lardoil with Sr: 0.33Al

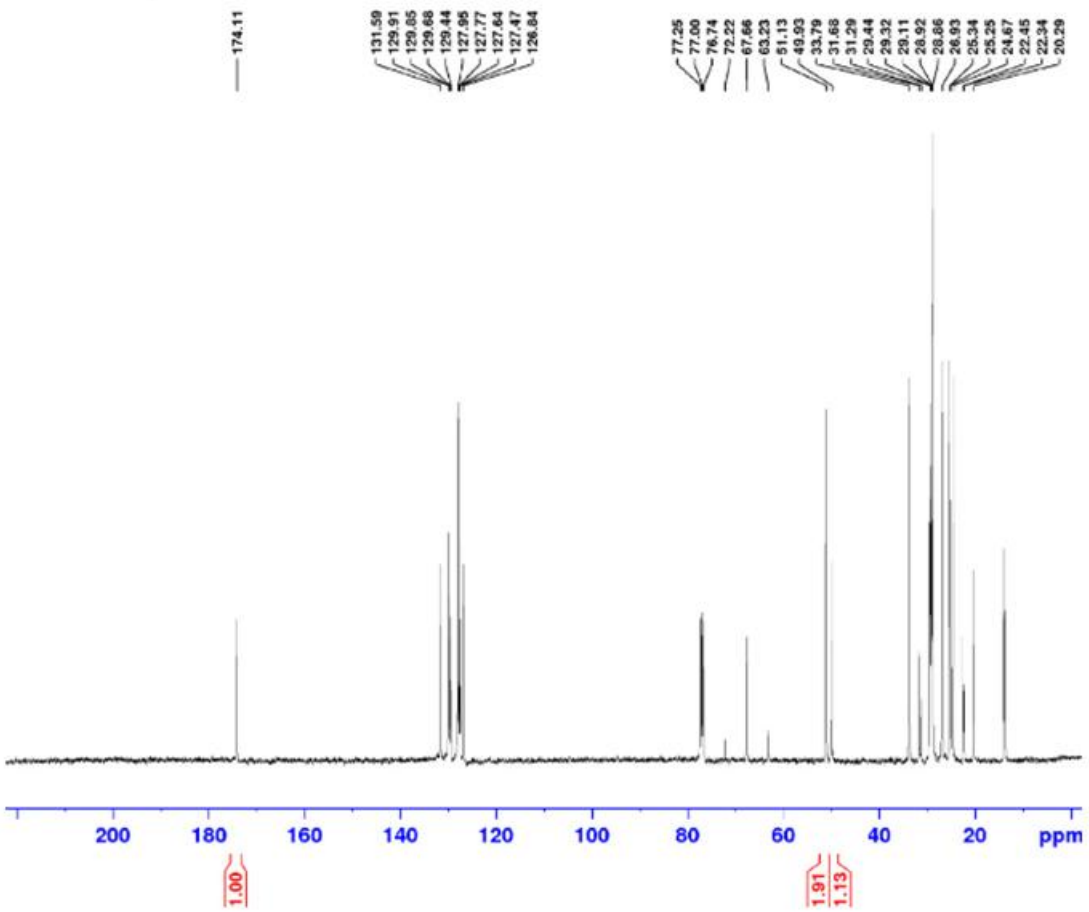

Fig S1 (b). The ^{13}C NMR for the biodiesel sample obtained from waste cooking oil with Sr: 0.33Al.